ENCLOSURE 2
TXX-92074

[redacted]

[redacted]

Westinghouse Energy Systems

WCAP-13168

TECHNICAL JUSTIFICATION FOR ELIMINATING 10" ACCUMULATOR LINES RUPTURE AS THE STRUCTURAL DESIGN BASIS FOR THE COMANCHE PEAK NUCLEAR PLANT UNIT 2

January 1992

Y. S. Lee
J. C. Schmertz
S. A. Swamy

Verified by: _____
F. J. Witt

Approved by: _____
D. C. Adamonis, Manager
Materials, Mechanics and Diagnostic Technology

Work Performed Under Shop Order: JJTP-5600

WESTINGHOUSE ELECTRIC CORPORATION
Nuclear and Advanced Technology Division
P.O. Box 2728
Pittsburgh, Pennsylvania 15230-2728

TABLE OF CONTENTS

TABLE OF CONTENTS (Cc..t'd.)

LIST OF TABLES

LIST OF TABLES (Cont'd.)

LIST OF FIGURES

LIST OF FIGURES (Cont'd.)

SECTION 1.0
INTRODUCTION

1.1 Background

The current structural design basis for the 10" accumulator lines requires postulating non-mechanistic circumferential and longitudinal pipe breaks. This results in additional plant hardware (e.g. pipe whip restraints and jet shields) which would mitigate the dynamic consequences of the pipe breaks. It is, therefore, highly desirable to be realistic in the postulation of pipe breaks for these lines and thereby eliminate the need for some of the plant hardware. Presented in this report are the descriptions of a mechanistic pipe break evaluation method and the analytical results that are used for establishing that a circumferential type break will not occur. The method applied is the leak-before-break procedure. The evaluations considering circumferentially oriented flaws envelop longitudinal cases.

1.2 Scope and Objective

The purpose of this investigation is to demonstrate leak-before-break for the 10" accumulator lines. The scope includes the entire accumulator lines, from the cold leg anchor point to the accumulator tank anchor point. Schematic drawings of the piping system are shown in section 3.0. The recommendations and criteria proposed in NUREG 1061 Volume 3 (1-1)* are used in this evaluation. These criteria and resulting steps of the evaluation procedure can be briefly summarized as follows:

1) Calculate the applied loads. Identify the location at which the highest stress occurs.

2) Identify the materials and the associated material properties.

---

* Numbers in parentheses refer to the references given at the end of the section.

3) Postulate a surface flaw. Determine fatigue crack growth. Show that a through-wall crack will not result.

4) Postulate a through-wall flaw at the governing location with the least favorable combination of stress and material properties. The size of the flaw should be large enough so that the leakage is assured of detection with margin using the installed leak detection equipment when the pipe is subjected to normal operating loads.

5) Using maximum faulted loads, demonstrate that there is a margin of at least 2 between the leakage size flaw and the critical size flaw.

6) Review the operating history to ascertain that operating experien has indicated no particular susceptibility to failure from the effects of corrosion, water hammer, or low and high cycle fatigue.

7) Justify that the material properties used in the evaluation are representative of the plant specific material. Evaluate long term effects such as thermal aging where applicable.

The flaw stability analysis is performed using the methodology described in SRP 3.6.3 (1-2).

The leak rates are calculated for the normal operating condition loads. The leak rate prediction model used in this evaluation is an [

]^{a,c,e} The crack opening area required for calculating the leak rates is obtained by subjecting the postulated through-wall flaw to normal operating loads (1-3). Surface roughness is accounted for in determining the leak rate through the postulated flaw.

The computer codes used in this evaluation for leak rate and fracture mechanics calculations have been validated (bench marked).

1.3 References

1-1 Report of the U.S. Nuclear Regulatory Commission Piping Review Committee - Evaluation of Potential for Pipe Breaks, NUREG 1061, Volume 3, November 1984.

1-2 Standard Review Plan; public comments solicited; 3.6.3 Leak-Before-Break Evaluation Procedures; Federal Register/Vol. 52, No. 167/Friday, August 28, 1987/Notices, pp. 32626-32633.

1-3 NUREG/CR-3464, 1983, "The Application of Fracture Proof Design Methods Using Tearing Instability Theory to Nuclear Piping Postulated Circumferential Through Wall Cracks."

SECTION 2.0
OPERATION AND STABILITY OF THE ACCUMULATOR LINES AND THE REACTOR COOLANT SYSTEM

2.1 Stress Corrosion Cracking

The Westinghouse type reactor coolant system primary loop and connecting Class 1 lines have an operating history that demonstrates the inherent operating stability characteristics of the design. This includes a low susceptibility to cracking failure from the effects of corrosion (e.g., intergranular stress corrosion cracking). This operating history totals over 450 reactor-years, including five plants each having over 17 years of operation and 15 other plants each with over 12 years of operation.

In 1976, the United States Nuclear Regulatory Commission (USNRC) formed the second Pipe Crack Study Group. (The first Pipe Crack Study Group established in 1975 addressed cracking in boiling water reactors only.) One of the objectives of the second Pipe Crack Study Group (PCSG) was to include a review of the potential for stress corrosion cracking in Pressurized Water Reactors (PWR's). The results of the study performed by the PCSG were presented in NUREG-0531 (2-1) entitled "Investigation and Evaluation of Stress Corrosion Cracking in Piping of Light Water Reactor Plants." In that report the PCSG stated:

> "The PCSG has determined that the potential for stress-corrosion cracking in PWR primary system piping is extremely low because the ingredients that produce IGSCC are not all present. The use of hydrazine additives and a hydrogen overpressure limit the oxygen in the coolant to very low levels. Other impurities that might cause stress-corrosion cracking, such as halides or caustic, are also rigidly controlled. Only for brief periods during reactor shutdown when the coolant is exposed to the air and during the subsequent startup are conditions even marginally capable of producing stress-corrosion cracking in the primary systems of PWRs. Operating experience in PWRs supports this determination. To date, no stress-corrosion cracking has been reported in the primary piping or safe ends of any PWR."

During 1979, several instances of cracking in PWR feedwater piping led to the establishment of the third PCSG. The investigations of the PCSG reported in NUREG-0691 (2-2) further confirmed that no occurrences of IGSCC have been reported for PWR primary coolant systems.

As stated above, for the Westinghouse type plants there is no history of cracking failure in the reactor coolant system loop or connecting Class 1 piping. The discussion below further qualifies the PCSG's findings.

For stress corrosion cracking (SCC) to occur in piping, the following three conditions must exist simultaneously: high tensile stresses, susceptible material, and a corrosive environment. Since some residual stresses and some degree of material susceptibility exist in any stainless steel piping, the potential for stress corrosion is minimized by properly selecting a material immune to SCC as well as preventing the occurrence of a corrosive environment. The material specifications consider compatibility with the system's operating environment (both internal and external) as well as other material in the system, applicable ASME Code rules, fracture toughness, welding, fabrication, and processing.

The elements of a water environment known to increase the susceptibility of austenitic stainless steel to stress corrosion are: oxygen, fluorides, chlorides, hydroxides, hydrogen peroxide, and reduced forms of sulfur (e.g., sulfides, sulphites, and thionates). Strict pipe cleaning standards prior to operation and careful control of water chemistry during plant operation are used to prevent the occurrence of a corrosive environment. Prior to being put into service, the piping is cleaned internally and externally. During flushes and preoperational testing, water chemistry is controlled in accordance with written specifications. Requirements on chlorides, fluorides, conductivity, and pH are included in the acceptance criteria for the piping.

During plant operation, the reactor coolant water chemistry is monitored and maintained within very specific limits. Contaminant concentrations are kept below the thresholds known to be conducive to stress corrosion cracking with the major water chemistry control standards being included in the plant operating procedures as a condition for plant operation. For example, during normal power operation, oxygen concentration in the RCS and connecting Class 1

lines is expected to be in the ppb range by controlling charging flow chemistry and maintaining hydrogen in the reactor coolant at specified concentrations. Halogen concentrations are also stringently controlled by maintaining concentrations of chlorides and fluorides within the specified limits. Thus during plant operation, the likelihood of stress corrosion cracking is minimized.

2.2 Water Hammer

Overall, there is a low potential for water hammer in the RCS and connecting accumulator lines since they are designed and operated to preclude the voiding condition in normally filled lines. The RCS and connecting accumulator lines including piping and components, are designed for normal, upset, emergency, and faulted condition transients. The design requirements are conservative relative to both the number of transients and their severity. Relief valve actuation and the associated hydraulic transients following valve opening are considered in the system design. Other valve and pump actuations are relatively slow transients with no significant effect on the system dynamic loads. To ensure dynamic system stability, reactor coolant parameters are stringently controlled. Temperature during normal operation is maintained within a narrow range by control rod position; pressure is controlled by pressurizer heaters and pressurizer spray also within a narrow range for steady-state conditions. The flow characteristics of the system remain constant during a fuel cycle because the only governing parameters, namely system resistance and the reactor coolant pump characteristics are controlled in the design process. Additionally, Westinghouse has instrumented typical reactor coolant systems to verify the flow and vibration characteristics of the system and connecting accumulator lines. Preoperational testing and operating experience have verified the Westinghouse approach. The operating transients of the RCS primary piping and connected accumulator lines are such that no significant water hammer can occur.

2.3 Low Cycle and High Cycle Fatigue

Low cycle fatigue considerations are accounted for in the design of the piping system through the fatigue usage factor evaluation to show compliance with the rules of Section III of the ASME Code. A further evaluation of the low cycle

fatigue loading is discussed in Section 6.0 as part of this study in the form of a fatigue crack growth analysis.

High cycle fatigue loads in the system would result primarily from pump vibrations during operation. During operation, an alarm signals the exceedance of the RC pump shaft vibration limits. Field measurements have been made on the reactor coolant loop piping of a number of plants during hot functional testing. Stresses in the elbow below the RC pump have been found to be very small, between 2 and 3 ksi at the highest. When translated to the connecting accumulator lines, these stresses are even lower, well below the fatigue endurance limit for the accumulator line material and would result in an applied stress intensity factor below the threshold for fatigue crack growth.

Vibratory fatigue loads are monitored for the 10-inch accumulator line during the hot-functional testing of the plant and are well below the high cycle fatigue allowables.

2.4 Potential Degradation During Service

Wall thinning by erosion and erosion-corrosion effects will not occur in the 10" accumulator line due to the low velocity, typically less than 10 ft/sec and the material, austenitic stainless steel, which is highly resistant to these degradation mechanisms.

The Comanche Peak Unit 2 accumulator lines nozzles are forged product forms which are not susceptible to toughness degradation due to thermal aging. Finally, the maximum operating temperature of the accumulator lines piping, which is about 560°F or below, is well below the temperature which would cause any creep damage in stainless steel piping.

2.5 References

2-1 Investigation and Evaluation of Stress-Corrosion Cracking in Piping of Light Water Reactor Plants, NUREG-0531, U.S. Nuclear Regulatory Commission, February 1979.

2-2 Investigation and Evaluation of Cracking Incidents in Piping in Pressurized Water Reactors, NUREG-0691, U.S. Nuclear Regulatory Commission, September 1980.

SECTION 3.0
MATERIAL CHARACTERIZATION

3.1 Pipe and Weld Materials

The materials of the accumulator lines are A376/TP316, A403/WP316, and A403/WP304. The injection nozzle material is SA351-CF8A, a cast product form of the type used for primary loop piping of several PWR plants. The accumulator line is connected to the primary loop at one end, and the other end is connected to the accumulator tank. The welding processes used are gas tungsten arc weld (GTAW), shielded metal arc weld (SMAW), and submerged arc weld (SAW). The normal operating pressure and temperature before the first valve from the cold leg are 2250 psia and 550°F, respectively. The pressure and temperature between the first and third valve are 2250 psia and 120°F. The pressure and temperature after the third valve are 700 psia and 120°F.

Weld locations and governing locations are identified in Figures 3-1 through 3-4 with the pipe geometries.

In the following sections the tensile properties of the materials are presented and criteria for use in the leak-before-break analyses are defined.

3.2 Material Properties of the Accumulator Lines

The room temperature mechanical properties of the Comanche Peak Unit 2 Nuclear Power Plant accumulator line materials were obtained from the Certified Materials Test Reports and are provided in Tables 3-1 through 3-4. The room temperature ASME Code (3-1) minimum properties are given in Table 3-5. It is seen that the measured properties well exceed those of the Code. The representative minimum and average tensile properties were established from the results given in Tables 3-1 through 3-4. The material properties at temperatures of 120°F and 550°F are required for the leak rate and stability analyses discussed later. The minimum and average tensile properties were calculated by using the ratio of the ASME Section III properties at the temperatures of interest stated above. Table 3-6 shows the tensile properties at the two temperatures of interest. The modulus of elasticity values were established at various temperatures from the ASME Section III (Table 3-7). In

the leak-before-break evaluation, the representative minimum properties at temperature are used for the flaw stability evaluations and the representative average properties are used for the leak rate predictions. Those properties are summarized in Table 3-6.

3.3 Tensile Properties of the Injection Nozzles

The material certifications for the injection nozzles were used to establish the tensile properties. These properties are given in Table 3-8 at room temperature.

From Table 3-8 the average yield strength value of SA351-CF8A [

]^{a,c,e} The modulus of elasticity was obtained from the Nuclear Systems Materials Handbook (reference 3-2) for consistency with the stress-strain diagram which was also obtained from that reference. The stress strain curve (minimum properties) is shown in Figure 3-5. This curve is used in the crack stability analyses.

3.4 Fracture Toughness Properties of the Injection Nozzles

Because the accumulator injection nozzle is a cast stainless steel product form operating at 550°F, thermal aging toughness degradation can take place. [

]^{a,c,e} the end of service life Charpy U-notch energy (KCU) following the procedure of reference (3-4). [ ]^{a,c,e}

[

].[a,c,e] By the criteria established in reference (3-3), the fracture toughness of the SA351-CF8A is at least as great as the toughness of [ ],[a,c,e] the benchmark material of reference (3-3).

Available data on aged stainless steel welds (reference (3-5)) indicate the J_{Ic} values for the worst case welds are of the same order as the aged [ ][a,c,e] material. However, the slope of the J-R curve is steeper, and higher J-values have been obtained from fracture tests (in excess of 3000 in-lb/in^2). The applied value of the J-integral for a flaw in the weld regions will be lower than that in the base metal because the yield stress for the weld materials is much higher at temperature. Therefore, weld regions are less limiting than the cast material.

Therefore, the toughness values for LBB evaluation are established as those of [ ][a,c,e]:

[ ][a,c,e]

3.5 References

3-1 ASME Boiler and Pressure Vessel Code Section III, Division 1, Appendices July 1, 1989.

3-2 Nuclear Systems Material Handbook, ERDA Report TID26666, November 1975, part I, Group 1, Section 4.

3-3 F. J. Witt and C. C. Kim, "Toughness Criteria for Thermally Aged Cast Stainless Steel," WCAP 10931, Revision 1, July 1986 (Westinghouse Proprietary Class 2).

3-4 Slama, G., Petrequin, P. , Masson, S. H., and Mager, T. R., "Effect of Aging on Mechanical Properties of Austenitic Stainless Steel Casting and Welds," presented at SMiRT 7 Post Conference Seminar 5 - Assuring Structural Integrity of Steel Reactor Pressure Boundary Components, August 29/30, 1983, Monterey, CA.

3-5 WCAP-10456, "The Effects of Thermal Aging on the Structural Integrity of Cast Stainless Steel Piping for W NSSS," W Proprietary Class 2, November 1983.

ROOM TEMPERATURE PROPERTIES OF THE ACCUMULATOR LINE MATERIALS FOR
LOOP 1 OF THE COMANCHE PEAK NUCLEAR POWER PLANT - UNIT 2

ID	Heat No./Serial No.	Material/Type	Yield Strength (psi)	Ultimate Strength (psi)	Elongation (%)	Area Red. (%)
A*	D5660	SA403/WP316	78,200	38,400	53.5	N/A **
B	3085-6-2	SA376/TP316	86,000	44,400	57.0	N/A
C	49201	SA403/WP316	80,000	51,000	61.5	N/A
D	3085-6-2	SA376/TP316	86,000	44,400	57.0	N/A
E	D5660	SA403/WP316	78,200	38,400	53.5	N/A
F	1081-21-1	SA376/TP316	83,050	43,050	57.0	N/A
G	53893	SA403/WP316	80,000	49,500	61.0	76.5
H	1081-21-1	SA376/TP316	83,050	43,050	57.0	N/A
I	49203	SA403/WP316	79,500	43,000	62.0	77.5
J	1081-21-1	SA376/TP316	83,050	43,050	57.0	N/A
K	53893	SA403/WP316	80,000	49,500	61.0	76.5
L	1081-21-1	SA376/TP316	83,050	49,500	57.0	N/A
M	1081-17-2	SA376/TP316	78,350	40,050	56.0	N/A
O	D4583	SA403/WP316	78,200	38,400	53.5	N/A
P	1081-9-1	SA376/TP316	79,600	41,050	63.0	N/A
Q	49199	SA403/WP316	82,500	52,500	56.0	73
R	1081-9-1	SA376/TP316	79,600	41,050	63.0	N/A
S	1081-18-1	SA376/TP316	80,000	42,350	60.0	N/A
T	53755	SA403/WP316	86,000	44,100	59.0	N/A
U	1081-18-1	SA376/TP316	80,000	42,350	60.0	N/A
V	53000	SA403/WP316	87,900	48,800	65.0	N/A

* As shown in Figure 3-1

** Not available

ROOM TEMPERATURE PROPERTIES OF THE ACCUMULATOR LINE MATERIALS FOR
LOOP 2 OF THE COMANCHE PEAK NUCLEAR POWER PLANT - UNIT 2

ID	Heat No./Serial No.	Material/Type	Yield Strength (psi)	Ultimate Strength (psi)	Elongation (%)	Area Red. (%)
A*	D5660	SA403/WP316	78,200	38,400	53.5	N/A **
B	3085-6-2	SA376/TP316	86,000	44,400	57.0	N/A
C	D5660	SA403/WP316	78,200	38,400	53.5	N/A
D	3085-6-2	SA376/TP316	86,000	44,400	57.0	N/A
E	D5660	SA403/WP316	78,200	38,400	53.5	N/A
F	3085-6-2	SA376/TP316	86,000	44,000	57.0	N/A
G	3085-4-2-2	SA316/TP316	83,200	44,500	66.0	75.5
H	55705	SA403/WP316	80,000	44,000	62.5	N/A
I	3085-4-2-2	SA376/TP316	83,200	44,500	66.0	N/A
J	54029	SA403/WP316	86,000	37,000	56.0	76.0
K	3085-4-2-2	SA376/TP316	83,200	44,500	66.0	N/A
L	55705	SA403/WP316	80,000	44,000	62.5	75.5
M	3085-4-2-2	SA376/TP316	83,200	44,500	66.0	N/A
N	1081-2-1	SA376/TP316	82,900	42,100	63.0	N/A
O	D5712	SA403/WP316	78,200	38,400	53.5	N/A
P	1081-18-1	SA376/TP316	80,000	42,350	60.0	N/A
Q	D4583	SA403/WP316	78,200	38,400	53.5	73
R	1081-19-1	SA376/TP316	81,750	42,500	61.0	N/A
S	D4583	SA403/WP316	78,200	38,400	53.5	N/A
T	1081-19-1	SA316/TP316	81,750	42,500	61.0	N/A
U	1081-19-1	SA376/TP316	81,750	42,500	61.0	N/A
V	53000	SA403/TP304	87,900	48,800	65.0	N/A

* As shown in Figure 3-2
** Not available

ROOM TEMPERATURE PROPERTIES OF THE ACCUMULATOR LINE MATERIALS FOR
LOOP 3 OF THE COMANCHE PEAK NUCLEAR POWER PLANT - UNIT 2

ID	Heat No./Serial No.	Material/Type	Yield Strength (psi)	Ultimate Strength (psi)	Elongation (%)	Area Red. (%)
A*	49201-4	SA403/WP316	80,000	51,000	61.5	N/A **
B	3085-4-2-2	SA376/TP316	83,200	44,500	66.0	N/A
C	49201-15	SA403/WP316	80,000	51,000	61.5	N/A
D	3085-4-2-2	SA376/TP316	83,200	44,500	66.0	N/A
E	49201-9	SA403/WP316	80,000	51,000	61.5	N/A
F	3085-4-2-2	SA376/TP316	83,200	44,500	66.0	N/A
G	3085-6-2	SA376/TP316	86,000	44,400	57.0	N/A
H	55706-1	SA403/WP316	77,500	42,000	62.0	75.5
I	3085-6-2	SA376/TP316	86,000	44,000	57.0	N/A
J	54029-1	SA403/WP316	86,000	37,000	56.0	76.0
K	3085-6-2	SA376/TP316	86,000	44,000	57.0	N/A
L	55706-2	SA403/WP316	77,500	42,000	62.0	75.5
M	3085-6-2	SA376/TP316	86,000	44,000	57.0	N/A
N	1081-14-2	SA376/TP316	87,250	49,000	47.0	N/A
O	D-5712	SA403/WP316	78,200	38,400	53.5	N/A
P	1081-14-2	SA376/TP316	82,750	49,000	47.0	N/A
Q	52975	SA403/WP316	80,000	52,500	61.0	74.5
R	1081-18-1	SA376/TP316	80,000	42,350	60.0	N/A
S	D-4583	SA403/WP316	78,200	38,400	53.5	N/A
T	3085-4-1	SA376/TP316	87,000	45,500	57.0	N/A
U	1081-14-1	SA376/TP316	81,150	44,150	64.0	N/A
V	53000	SA403/WP304	87,900	48,000	65.0	N/A

* As shown in Figure 3-2
** Not available

ROOM TEMPERATURE PROPERTIES OF THE ACCUMULATOR LINE MATERIALS FOR
LOOP 4 OF THE COMANCHE PEAK NUCLEAR POWER PLANT - UNIT 2

ID	Heat No./Serial No.	Material/Type	Yield Strength (psi)	Ultimate Strength (psi)	Elongation (%)	Area Reduction (%)
A*	55705-2	SA403/WP316	80,000	44,000	62.5	75.5
B	3085-6-2	SA376/TP316	86,000	44,400	57.0	N/A **
C	55705-1	SA403/WP316	80,000	44,000	62.5	75.5
D	3085-6-2	SA376/TP316	86,000	44,400	57.0	N/A
E	55705-5	SA403/WP316	80,000	44,000	62.5	75.5
F	3085-6-2	SA376/TP316	86,000	44,400	57.0	N/A
G	1081-2-2-1	SA376/TP316	82,900	42,100	63.0	76.5
H	53893-2	SA403/WP316	80,000	49,500	61.0	N/A
I	1081-2-2-1	SA376/TP316	82,900	42,100	63.0	77.5
J	49203	SA403/WP316	79,500	43,000	62.0	N/A
K	1081-21-1	SA376/TP316	83,050	43,050	57.0	N/A
L	53893-4	SA403/WP316	80,000	49,500	61.0	N/A
M	1081-2-2-1	SA376/TP316	82,900	42,100	63.0	N/A
N	1081-19-2	SA376/TP316	79,600	41,050	63.0	N/A
O	D4583	SA403/WP316	78,200	38,400	53.5	N/A
P	1081-2-1	SA376/TP316	82,900	42,100	63.0	N/A
Q	53755	SA403/WP316	86,000	44,100	59.0	N/A
R	1081-2-1	SA376/TP316	82,900	42,100	63.0	N/A
S	1081-9-1	SA376/TP316	79,600	41,050	63.0	N/A
T	49778	SA403/WP304	85,600	44,900	61.0	N/A

* As shown in Figure 3-4

** Not available

TABLE 3-5

Room Temperature ASME Code Minimum Properties

Material	Yield Stress (psi)	Ultimate Stress (psi)
A403/WP304	30,000	75,000
A376/TP316 and A403/WP316	30,000	75,000

TABLE 3-6

Tensile Properties for the Comanche Peak Unit 2 Nuclear Power Plant
10" Accumulator Lines

Material	Temperature (°F)	Minimum Yield (psi)	Average Yield (psi)	Minimum Ultimate (psi)
A403/WP304	120	43,417	46,052	85,285
A376/TP316	120	38,727	42,997	78,062
	550	23,027	25,567	60,413
A403/WP316	120	35,778	40,827	77,214
	550	23,538	26,860	63,734
SA351/CF8A	550	22,178	25,318	70,465

TABLE 3-7

Modulus of Elasticity (E)

Temperature (°F)	E (ksi)
120	28,031
550	25,550

AVAILABLE MECHANICAL PROPERTIES OF THE
ACCUMULATOR INJECTION NOZZLES AT ROOM TEMPERATURE

Loop No.	Product Form	Heat Number	Material	0.2% Offset Yield Stress (psi)	Ultimate Strength (psi)	% Elongation per Inch	% Reduction in Area
1	Nozzle	3-3659/0763	SA351-CF8A	35124	82085	62.0	N/A
2	Nozzle	3-3698/1154	SA351-CF8A	41398	85640	59.0	N/A
3	Nozzle	3-3719/3333	SA351-CF8A	42180	89269	59.6	N/A
4	Nozzle	3-3695/0762	SA351-CF8A	41682	88458	56.2	N/A

N/A - Not available

TABLE 3-9

CHEMISTRY AND END OF SERVICE LIFE KCU TOUGHNESS
FOR ACCUMULATOR INJECTION NOZZLES

Heat No.	Cr %	Si %	Ni %	Mo %	C %	Mn %	N %	Cb %	KCU daJ/cm^2
3-3659/0763									a,c,e
3-3698/1154									
3-3719/3333									
3-3695/0762									

Pipe Outside Diameter 10.75 in.
Minimum Wall Thickness 0.875 in.
Accumulator Tank Nozzle Safe End:
Minimum Wall Thickness 0.3285 in.
SW - Shop Weld
FW - Field Weld

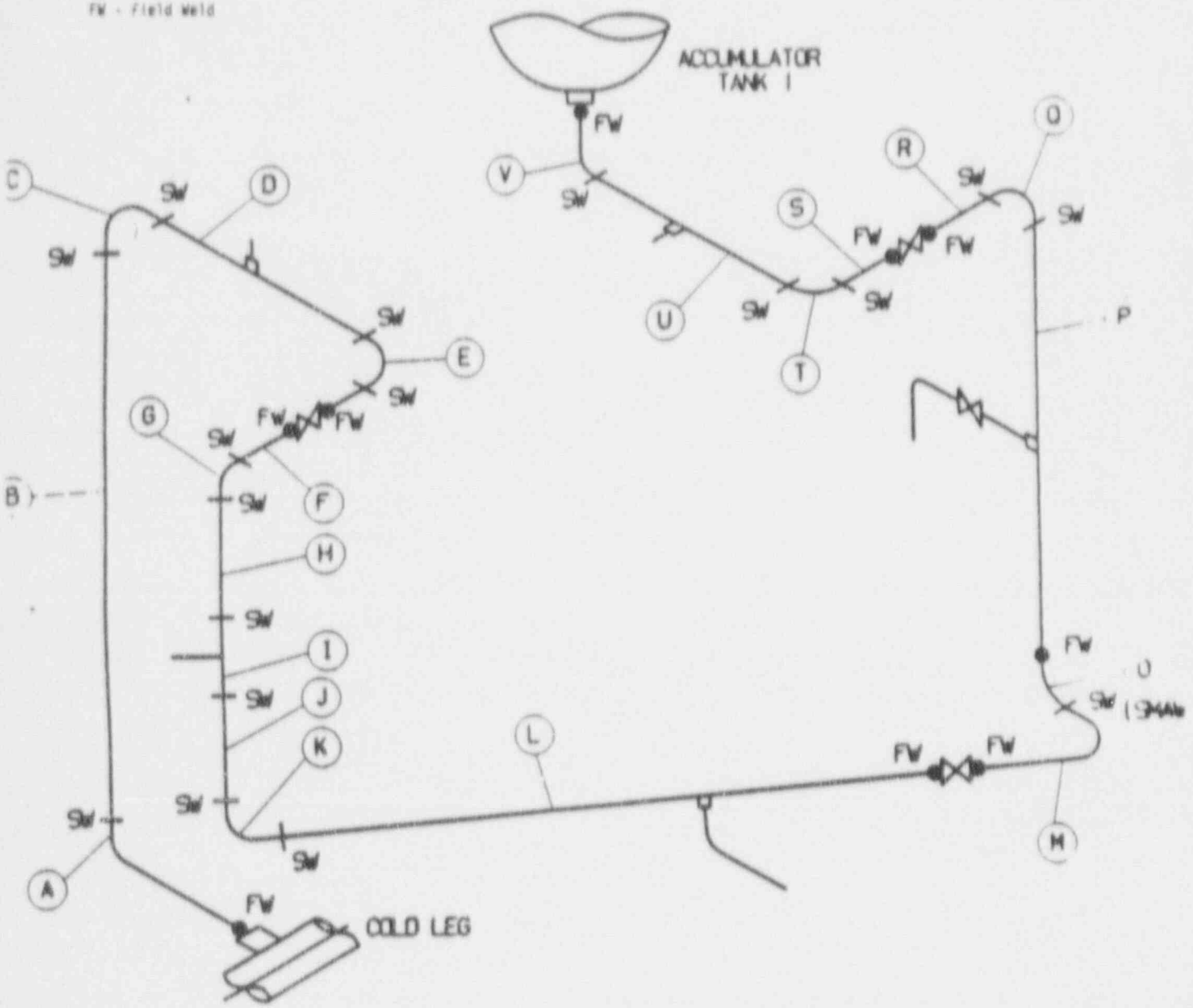

Figure 3-1. Layout of the Accumulator Line for Loop 1

Pipe Outside Diameter 10.75 in.
Minimum Wall Thickness 0.875 in.
Accumulator Tank Nozzle Safe End:
Minimum Wall Thickness 0.3285 in.
SW - Shop Weld
FW - Field Weld

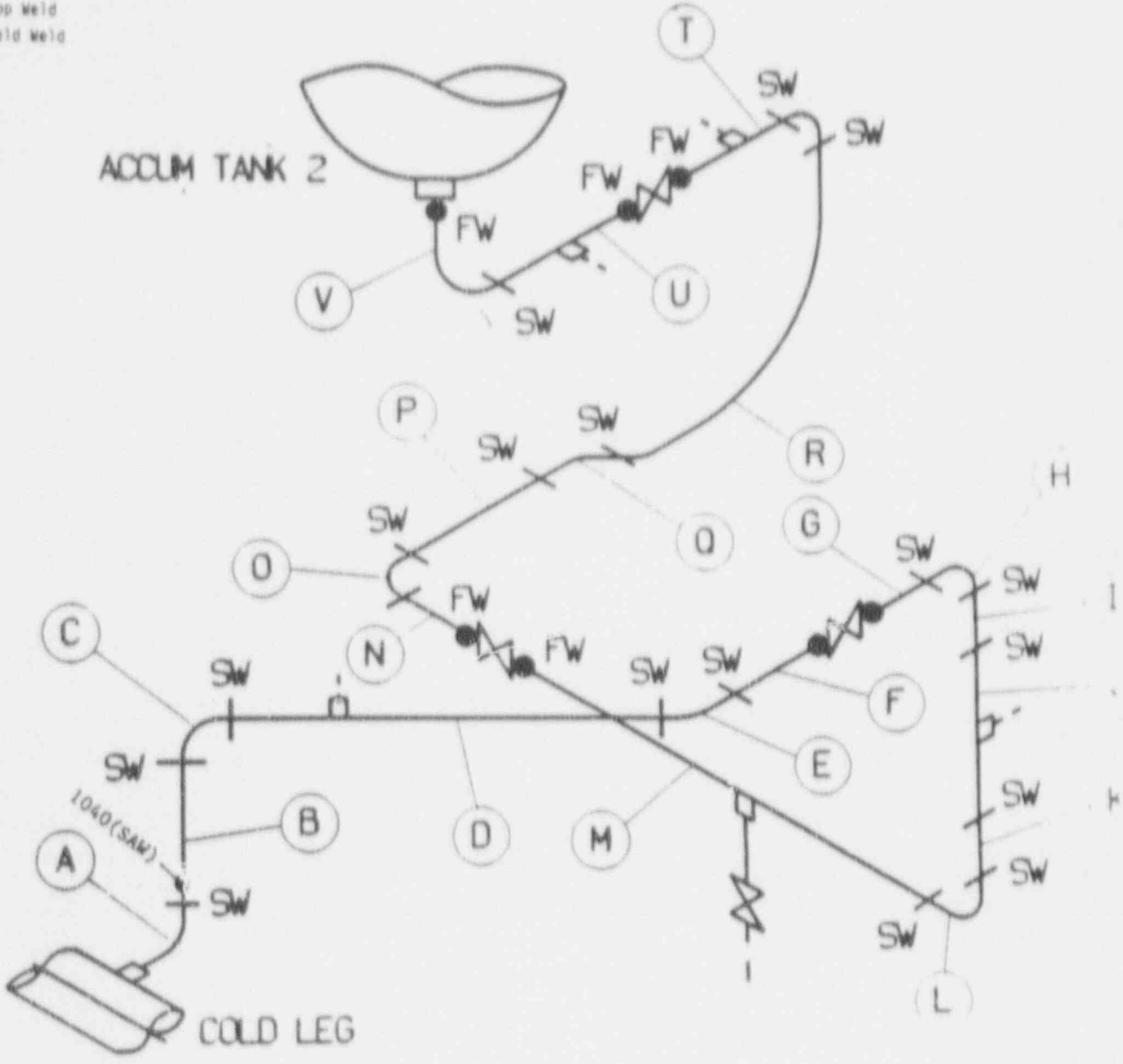

Figure 3-2. Layout of the Accumulator Line for Loop 2

Pipe Outside Diameter 10.75 in.
Minimum Wall Thickness 0.875 in.
Accumulator Tank Nozzle Safe End:
Minimum Wall Thickness 0.3285 in.
SW - Shop Weld
FW - Field Weld

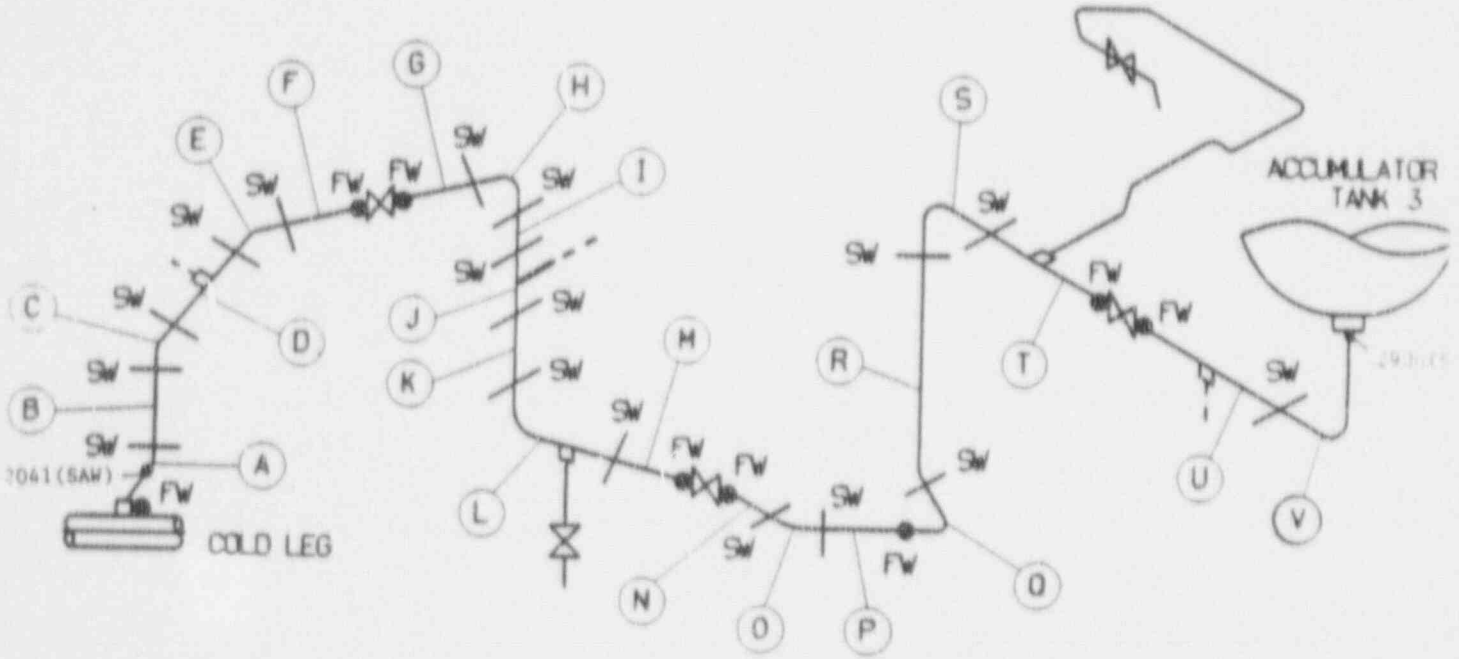

Figure 3-3. Layout of the Accumulator Line for Loop 3

Pipe Outside Diameter 10.75 in.
Minimum Wall Thickness 0.875 in.
Accumulator Tank Nozzle Safe End:
Minimum Wall Thickness 0.3285 in.
SW - Shop Weld
FW - Field Weld

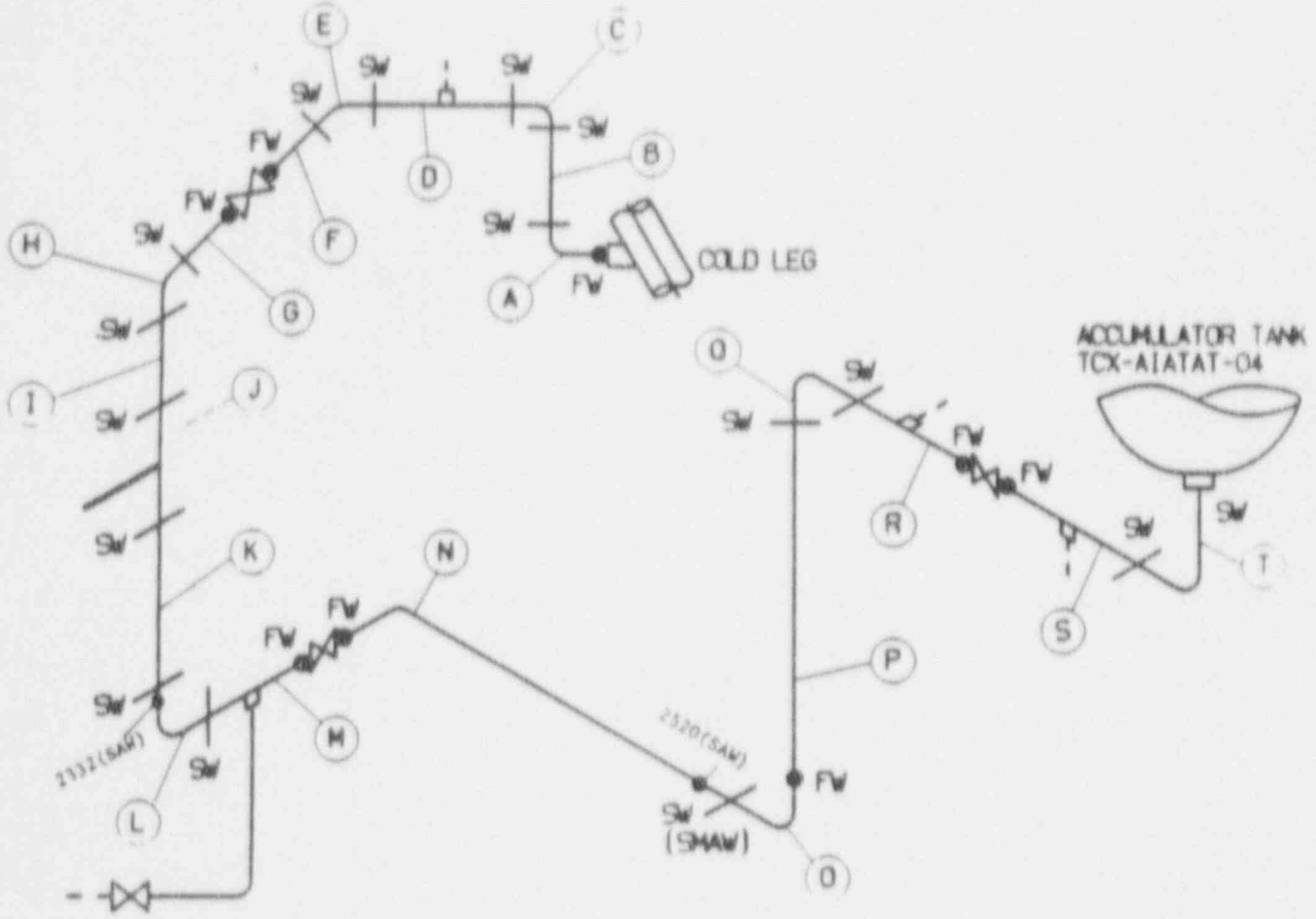

Figure 3-4. Layout of the Accumulator Line for Loop 4

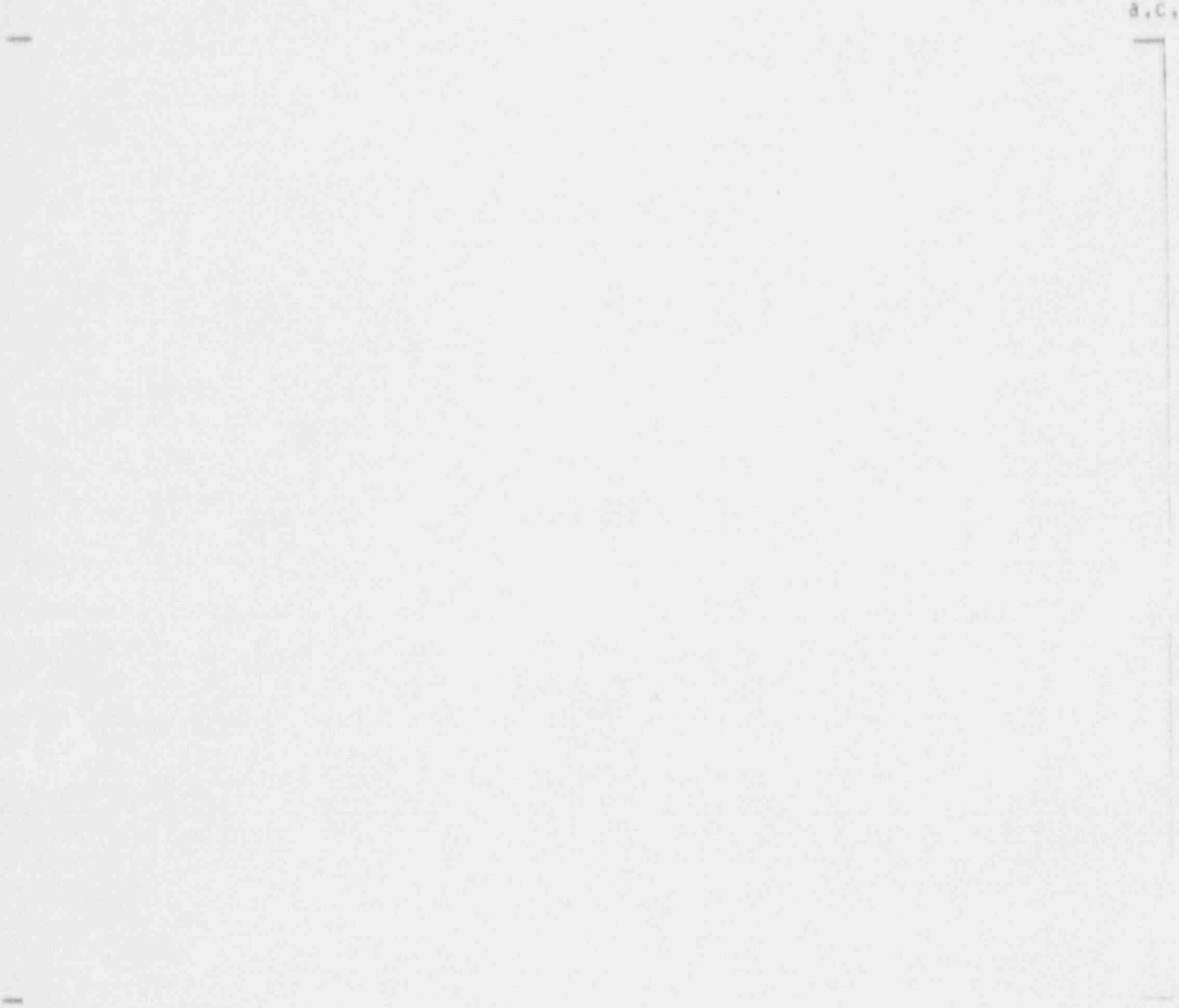

Figure 3-5. True Stress Strain Curve for SA351-CF8A Stainless Steel at 550°F

SECTION 4.0
LOADS FOR FRACTURE MECHANICS ANALYSIS

4.1 Nature of the Loads

Under normal operating conditions, the accumulator lines are subjected to axial and bending loads which arise from deadweight, pressure, and thermal expansion. Under faulted conditions, the loads caused by Safe Shutdown Earthquake (SSE) are superimposed on these normal operating loads.

The stresses due to axial loads and bending moments were calculated by the following equation:

$$\sigma = \frac{F}{A} + \frac{M}{Z} \qquad (4\text{-}1)$$

where,

σ	=	stress
F	=	axial load
M	=	bending moment
A	=	pipe cross-sectional area
Z	=	section modulus

The x direction is the axial direction of the pipe with y and z denoting the remaining orthogonal directions. The bending moments for the desired loading combinations were calculated by the following equation:

$$M = (M_Y^2 + M_Z^2)^{1/2} \qquad (4\text{-}2)$$

where,

M	=	bending moment for required loading
M_Y	=	y component of bending moment
M_Z	=	z component of bending moment

The axial load and bending moments for crack stability analysis and leak rate predictions were computed by the methods explained in Sections 4.1 and 4.2 which follow.

4.2 Loads for Crack Stability Analysis

The faulted loads for the crack stability analysis were calculated by the absolute sum method as follows:

$$F = |F_{DW}| + |F_{TH}| + |F_P| + |F_{SSE}| \quad (4\text{-}3)$$

$$M_Y = |(M_Y)_{DW}| + |(M_Y)_{TH}| + |(M_Y)_{SSE}| \quad (4\text{-}4)$$

$$M_Z = |(M_Z)_{DW}| + |(M_Z)_{TH}| + |(M_Z)_{SSE}| \quad (4\text{-}5)$$

Where, the subscripts of the above equations represent the following loading cases:

DW = deadweight
TH = normal thermal expansion
SSE = SSE loading including seismic anchor motion
P = load due to internal pressure

4.3 Loads for Leak Rate Evaluation

The normal operating loads for leak rate predictions were calculated by the algebraic sum method as follows:

$$F = F_{DW} + F_{TH} + F_P \quad (4\text{-}6)$$

$$M_Y = (M_Y)_{DW} + (M_Y)_{TH} \quad (4\text{-}7)$$

$$M_Z = (M_Z)_{DW} + (M_Z)_{TH} \quad (4\text{-}8)$$

The parameters and the subscripts are the same as those explained in Section 4.2.

4.4 Summary of Loads and Geometry

The load combinations were evaluated at the various weld locations. Normal loads were determined using the algebraic sum method whereas faulted loads were combined using the absolute sum method as discussed above.

4.5 Governing Locations

The governing locations were established on the basis of the pipe schedules, types of material, operating temperature, material properties, the highest faulted stresses for the welds, and the types of welds. The shop welds (SW) were SAW and the field welds (FW) were made by the combination of GTAW and SMAW. Maximum faulted loads of the node point in the neighborhood of the nozzles were used for the loads of the injection nozzles. This node was identified as node 2041 in loop 3. All four loops were investigated and the following governing locations were identified:

Material	Temperature (°F)	Node
SA351/CF8A	550	2041/Loop 3
SA403/TP316	550	2041/Loop 3
	120	2332/Loop 4
SA376/TP316	550	1040/Loop 2
	120	2520/Loop 4
SA403/TP304	120	2900/Loop 3

The loads and stresses for the governing locations are shown in Table 4-1. In developing these tables the appropriate wall thicknesses were used.

The governing locations have been indicated in the layout sketches of Figures 3-2, 3-3 and 3-4.

TABLE 4-1

Summary of Normal and Faulted Loads and Stresses at Governing Locations

Node & Loop	Load Case	Axial Force* (lbs)	Axial Stress (psi)	Bending Moment (in-lbs)	Bending Stress (psi)	Total Stress (psi)
2041/3	Normal	129,137	4,757	361,541	5,827	10,584
	Faulted	147,316	5,427	950,338	15,317	20,744
1040/2	Normal	127,385	4,693	392,791	6,331	11,024
	Faulted	147,362	5,429	618,966	9,976	15,404
2332/4	Normal	139,243	5,130	342,416	5,519	10,648
	Faulted	151,284	5,573	744,449	11,999	17,572
2520/4	Normal	136,521	5,029	488,785	7,878	12,907
	Faulted	139,630	5,144	1,066,744	17,193	22,337
2900/3	Normal	55,955	5,202	50,155	1,844	7,047
	Faulted	58,185	5,410	233,841	8,600	14,010

* Pressure included.

SECTION 5.0
FRACTURE MECHANICS EVALUATION

5.1 Failure Mechanism

Determination of the conditions which lead to failure should be done with plastic fracture methodology because of the large amount of deformation accompanying fracture. One method for predicting the failure of ductile material is the [ ]^{a,c,e} method, based on traditional plastic limit load concepts, but accounting for [ ]^{a,c,e} and taking into account the presence of a flaw. The flawed pipe is predicted to fail when the remaining net section reaches a stress level at which a plastic hinge is formed. The stress level at which this occurs is called the flow stress. [

]^{a,c,e}

This methodology has been shown to be applicable to ductile piping through a large number of experiments and is used here to predict the critical flaw sizes in the accumulator lines. The failure criterion has been obtained by requiring equilibrium of the section containing the flaw (Figure 5-1) when loads are applied. The detailed development is provided in Appendix A for a through- wall circumferential flaw in a pipe with internal pressure, axial force, and imposed bending moments. The limit moment for such a pipe is given by: [ ]^{a,c,e} (5-1)

with

[ ]^{a,c,e} (5-2)

where:

[

]^{a,c,e}

[

]^{a,c,e}

The analytical model described above accurately accounts for the piping internal pressure as well as imposed axial force as they affect the limit moment. Good agreement was found between the analytical predictions and the experimental results (5-1). Flaw stability evaluations using this analytical model, are presented in section 5.3.

5.2 Leak Rate Predictions

The purpose of this section is to discuss the method which will be used to predict the flow through a postulated crack and present the leak rate calculation results for postulated through-wall circumferential cracks in the accumulator lines.

5.2.1 General Considerations

The flow of hot pressurized water through an opening to a lower back pressure (causing choking) is taken into account. For long channels where the ratio of the channel length, L, to hydraulic diameter, D_H, (L/D_H) is greater than [ ]^{a,c,e}, both [ ]^{a,c,e} must be considered. In this situation the flow can be described as being single-phase through the channel until the local pressure equals the saturation pressure of the fluid. At this point, the flow begins to flash and choking occurs. Pressure losses due to momentum changes will dominate for [ ]^{a,c,e} However, for large L/D_H values, friction pressure drop will become important and must be considered along with the momentum losses due to flashing.

5.2.2 Calculation Method

Using an [

]^{a,c,e}

The flow rate through a crack was calculated in the following manner. Figure 5-2 from reference 5-2 was used to estimate the critical pressure, Pc, for the primary loop enthalpy condition and an assumed flow. Once Pc was found for a given mass flow, the [ ]^{a,c,e} was found from Figure 5-3 taken from reference 5-2. For all cases considered, since [ ]^{a,c,e} Therefore, this method will yield the two-phase pressure drop due to momentum effects as illustrated in Figure 5-4. Now using the assumed flow rate, G, the frictional pressure drop can be calculated using

$$\Delta P_f = [\quad]^{a,c,e} \qquad (5\text{-}3)$$

where the friction factor f is determined using the [ ]^{a,c,e} The crack relative roughness, e, was obtained from fatigue crack data on stainless steel samples. The relative roughness value used in these calculations was [ ]^{a,c,e} RMS.

The frictional pressure drop using equation 5-3 is then calculated for the assumed flow and added to the momentum pressure drop calculated using the Fauske model to obtain the total pressure drop from the primary system to the atmosphere. Thus,

$$\text{Absolute Pressure} - 14.7 = [\quad]^{a,c,e} \qquad (5\text{-}4)$$

for a given assumed flow G. If the right-hand side of equation 5-4 does not agree with the pressure difference between the piping under consideration and the atmosphere, then the procedure is repeated until equation 5-4 is satisfied to within an acceptable tolerance and this results in the flow value through the crack.

For the locations at the lower temperature, single phase calculations for the leak rate in gallons per minute (GPM) were performed, using an equation from reference 5-3 as follows:

$$[\quad]^{a,c,e} \qquad (5\text{-}5)$$

[

]a,c,e

5.2.3 Leak Rate Calculations

Leak rate calculations were made as a function of postulated through-wall crack length for the five critical locations previously identified. The crack opening areas were estimated using the method of reference 5-4 and the leak rates were calculated using the calculational methods described above. The leak rates were calculated using the normal operating loads at the governing nodes identified in section 4.0. The crack lengths yielding a leak rate of 10 gpm (10 times the leak detection capability of 1.0 gpm) for the critical locations at the Comanche Peak Nuclear Power Plant Unit 2 are shown in Table 5-1.

5.2.4 Leak Detection Capability

The Comanche Peak Unit 2 Nuclear Power Plant leak detection system inside the containment can detect 1 gpm leak rates as required by Regulatory Guide 1.45. As seen above, a margin of 10 was applied to the leak rate to define the accumulator line leakage size flaws in accordance with NUREG 1061, Volume 3.

5.3 Stability Evaluation of Accumulation Lines

A typical segment of a pipe under maximum loads of axial force F and bending moment M is schematically illustrated as shown in Figure 5-5. In order to calculate the critical flaw size, plots of the limit moment versus crack length are generated as shown in Figures 5-6 through 5-10. As mentioned in

Section 4.0, shop welds were performed by SAW and field welds were performed by the combination of GTAW and SMAW. Therefore field weld locations are conservatively considered to be SMAW. The nodes of maximum load under faulted condition are found to be all shop weld (SW) and therefore the leak-before-break concept is demonstrated for SAW welding procedures. The critical flaw size corresponds to the intersection of the limit moment curve and the maximum moment load line. The critical flaw size is calculated using the lower bound base metal tensile properties established in section 3.0.

The "Z" factor correction for SAW weld was applied (5-5 and 5-6) as follows:

$$Z = 1.30\ [1 + 0.010\ (OD - 4)] \qquad (5\text{-}6)$$

where OD is the outer diameter in inches. Substituting OD=10.75 inches, the Z factor was calculated to be 1.39 for SAW. The applied loads at the SAW locations were increased by the Z factors and the plots of limit load versus crack length were generated as shown in Figure 5-6 to 5-10. Table 5-2 shows the summary of critical flaw sizes for the Comanche Peak Unit 2 nuclear power plant 10" accumulator lines.

5.4 Local Stability Analysis of the Injection Nozzles

In this section the local stability analysis is performed to show that unstable crack extension will not occur when postulated through wall flaws in the cast injection nozzles are subjected to maximum loads.

At the critical nozzle identified in Section 3.0, the (normal plus SSE) outer surface axial stress, σ_a, is seen to be 20.7 ksi based on the minimum wall thickness (see Table 4-1 of Section 4.0). The (normal plus SSE) axial force and bending moment are Fx = 147 kips and M_b = 950.3 in-kips.

The minimum yield strength for flaw stability analysis is 22.2 ksi (see Section 3.0). The EPRI elastic-plastic fracture handbook method was used to calculate the J_{app} using the normal plus SSE loads. The J_{app} was calculated for a [ ]^{a,c,e} long postulated through wall flaw (which is 2 times the reference flaw size) and was found to be [ ]^{a,c,e}. Since the J_{app} value is greater than the J_{1c} value of [ ]^{a,c,e} the tearing modulus

was evaluated. The applied tearing modulus, T_{app} was found to be [ ]^{a,c,e}. Both J_{app} and T_{app} are below the allowables of [ ]^{a,c,e}, respectively, given in Section 3.0. Therefore, unstable crack propagation will not result.

5.5 References

5-1 Kanninen, M. F. et al., "Mechanical Fracture Predictions for Sensitized Stainless Steel Piping with Circumferential Cracks" EPRI NP-192, September 1976.

5-2 [

]^{a,c,e}

5-3 "Thermal Engineering," C. C. Dillio and E.P. Nye, International Text Company, pp. 270-273, 1969.

5-4 Tada, H., "The Effects of Shell Corrections on Stress Intensity Factors and the Crack Opening Area of Circumferential and a Longitudinal Through-Crack in a Pipe," Section II-1, NUREG/CR-3464, September 1983.

5-5 ASME Code Section XI, Winter 1985 Addendum, Article IWB-3640.

5-6 Standard Review Plan; Public Comment Solicited; 3.6.3 Leak-Before-Break Evaluation Procedures; Federal Register/Vol. 52, No. 167/Friday, August 28, 1987/Notices, pp. 32626-32633.

TABLE 5-1

Leak Rate Crack Lengths for the Governing Locations of Comanche Peak Unit 2 Accumulator Lines

Node Point	Material	Location	Temperature (°F)	Crack Length (in.) (for 10 gpm leakage)
[				] a,c,e

* Before the first valve from RCS (t = 0.875 in.)

** After the first valve from RCS (t = 0.875 in.)

*** Accumulator tank nozzle junction (t = 0.3285 in.)

TABLE 5-2

Summary of Critical Flaw Sizes for the Governing Locations of the Comanche Peak Unit 2 10" Accumulator Lines

Node Point	Material	Location	Temperature (°F)	Critical Flaw Size (in.) SAW
[				] a,c,e

Figure 5-1 Fully Plastic Stress Distribution

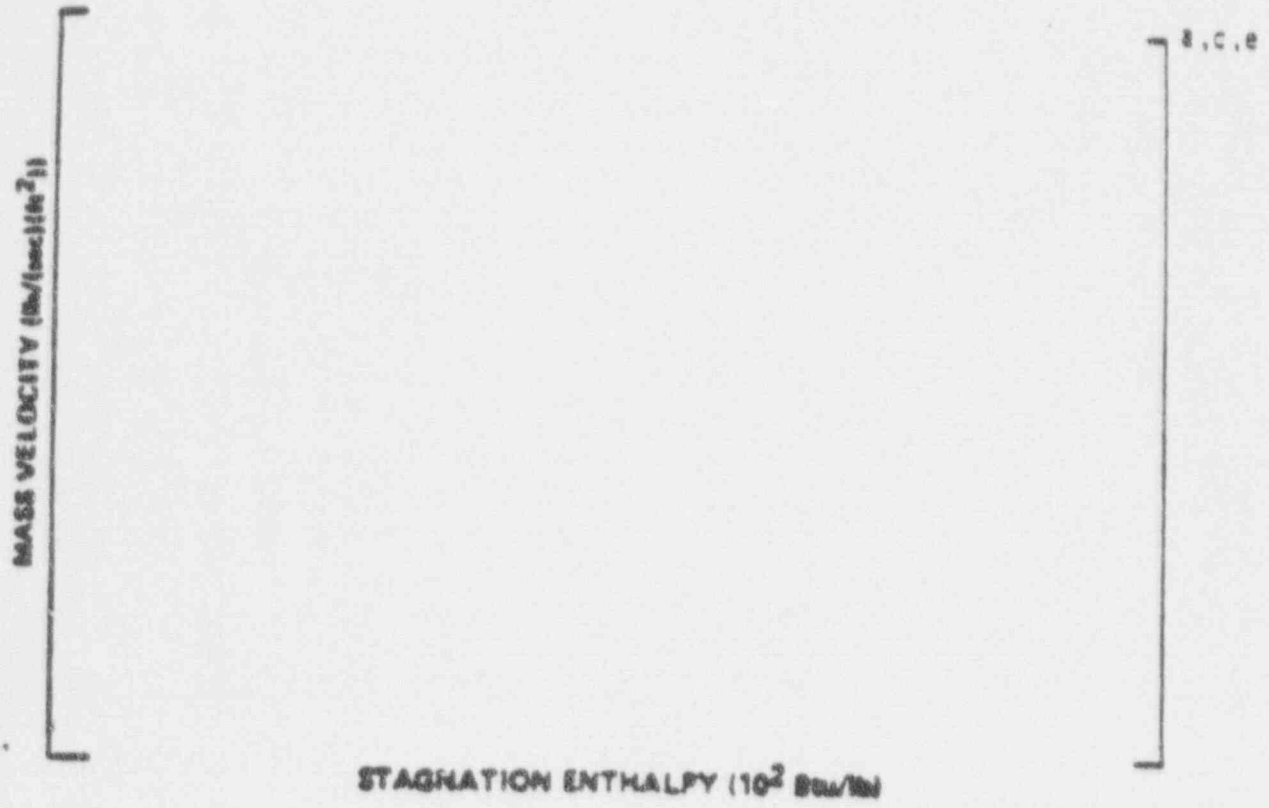

Figure 5-2. Analytical Predictions of Critical Flow Rates of Steam-Water Mixtures

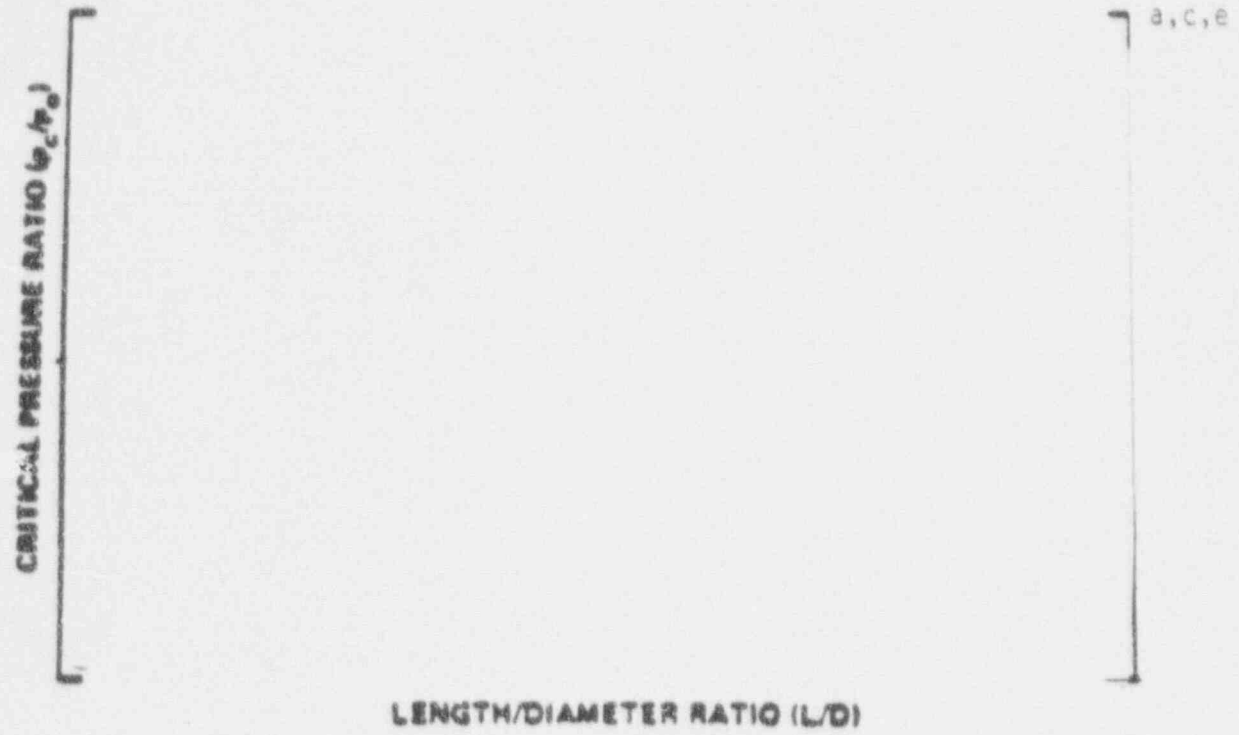

Figure 5-3. [ ]^{a,c,e} Pressure Ratio as a Function of L/D

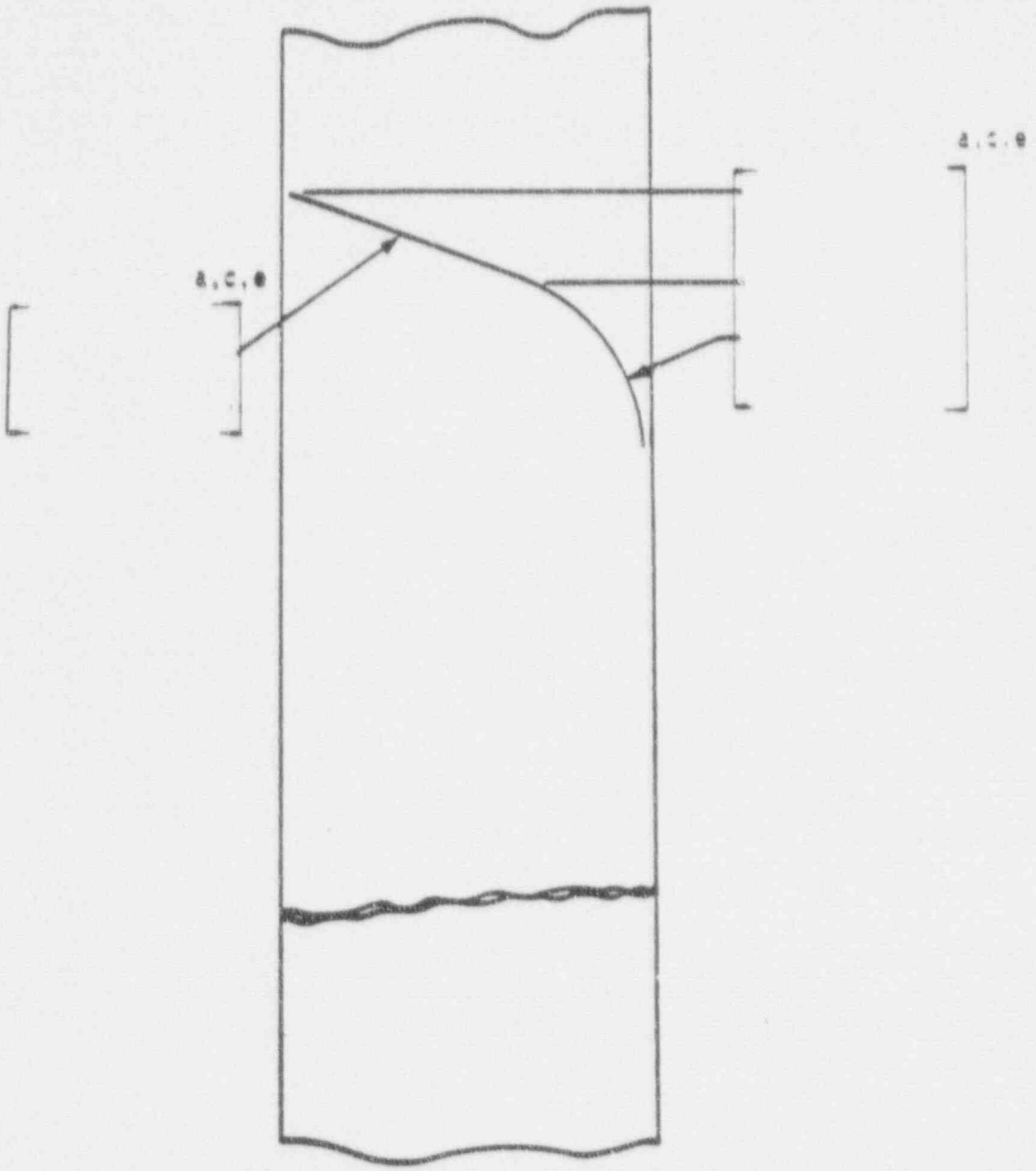

Figure 5-4. Idealized Pressure Drop Profile Through a Postulated Crack

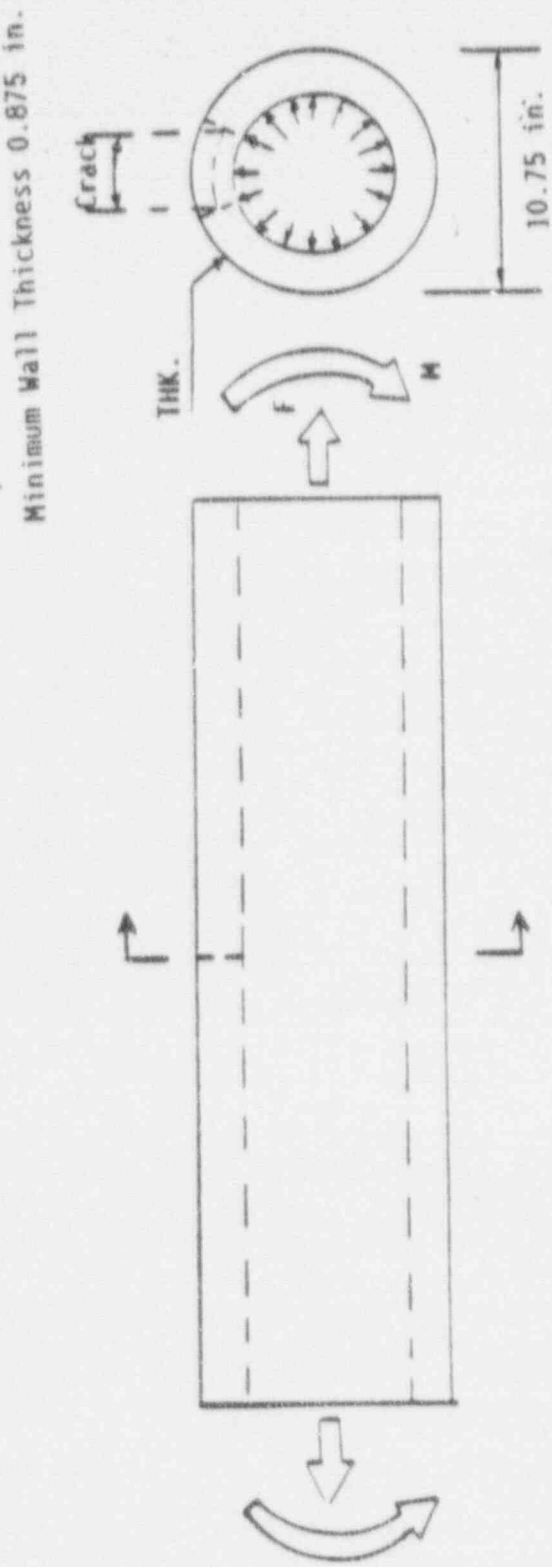

Figure 5-5. Loads Acting on a Pipe Model

a,c,e

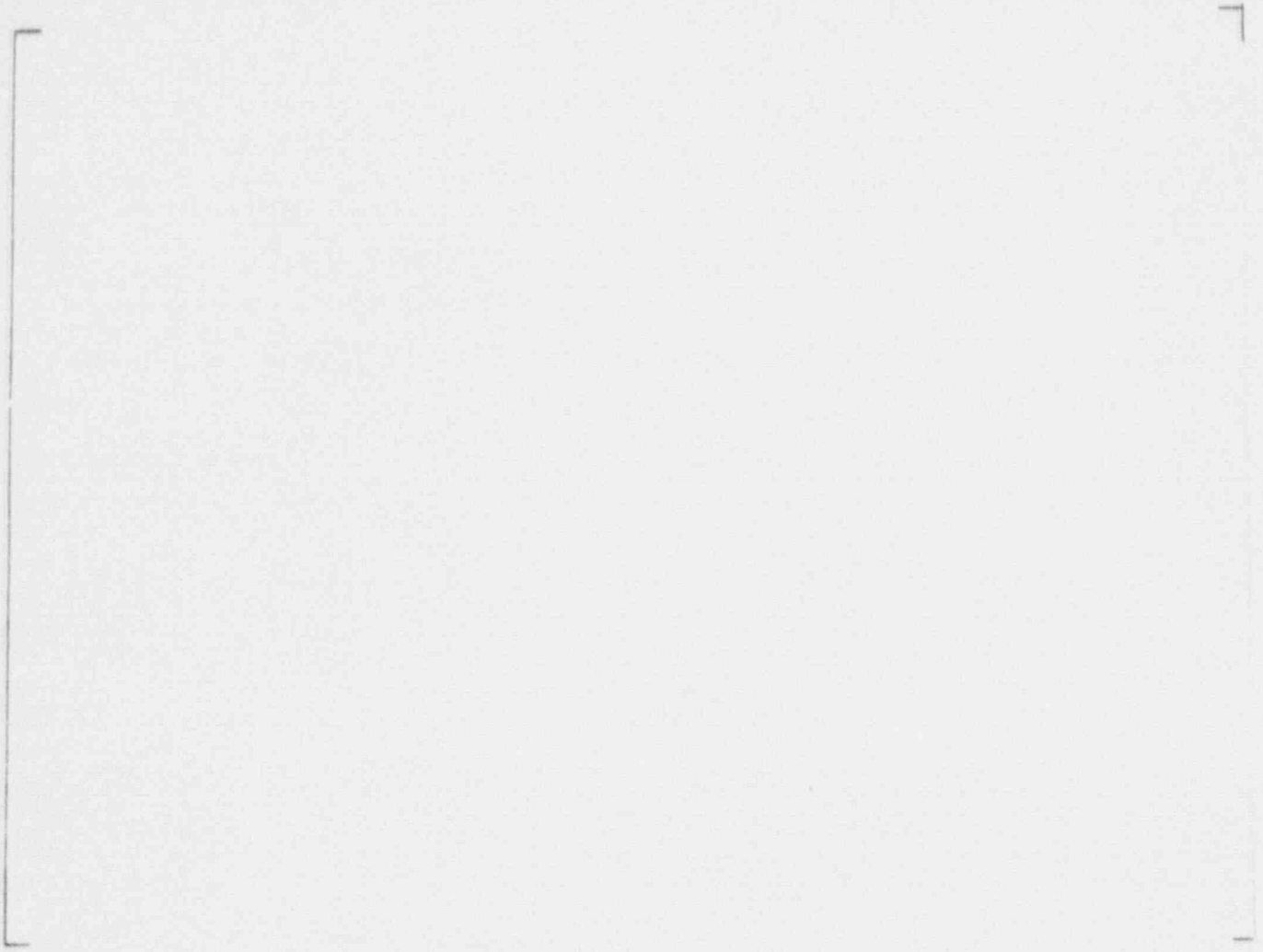

Figure 5-6. Critical Flaw Size Prediction for the Comanche Peak Nuclear Power Plant Node 2041 - SAW

a,c,e

Figure 5-7. Critical Flaw Size Prediction for the Comanche Peak Nuclear Power Plant Node 1040 - SAW

a,c,e

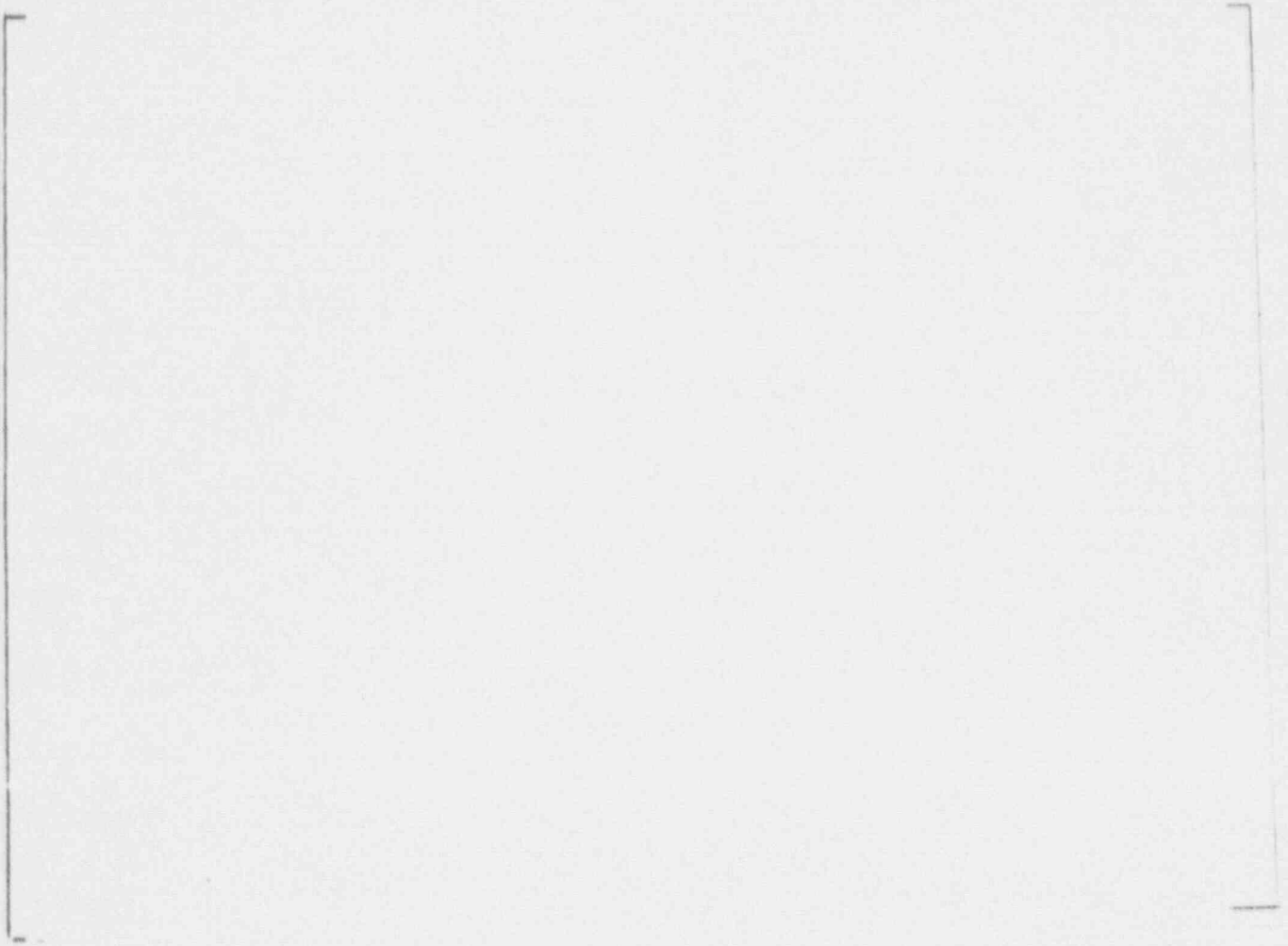

Figure 5-8. Critical Flaw Size Prediction for the Comanche Peak Nuclear Power Plant Node 2332 - SAW

Figure 5-9. Critical Flaw Size Prediction for the Comanche Peak Nuclear Power Plant Node 2520 - SAW

a,c,e

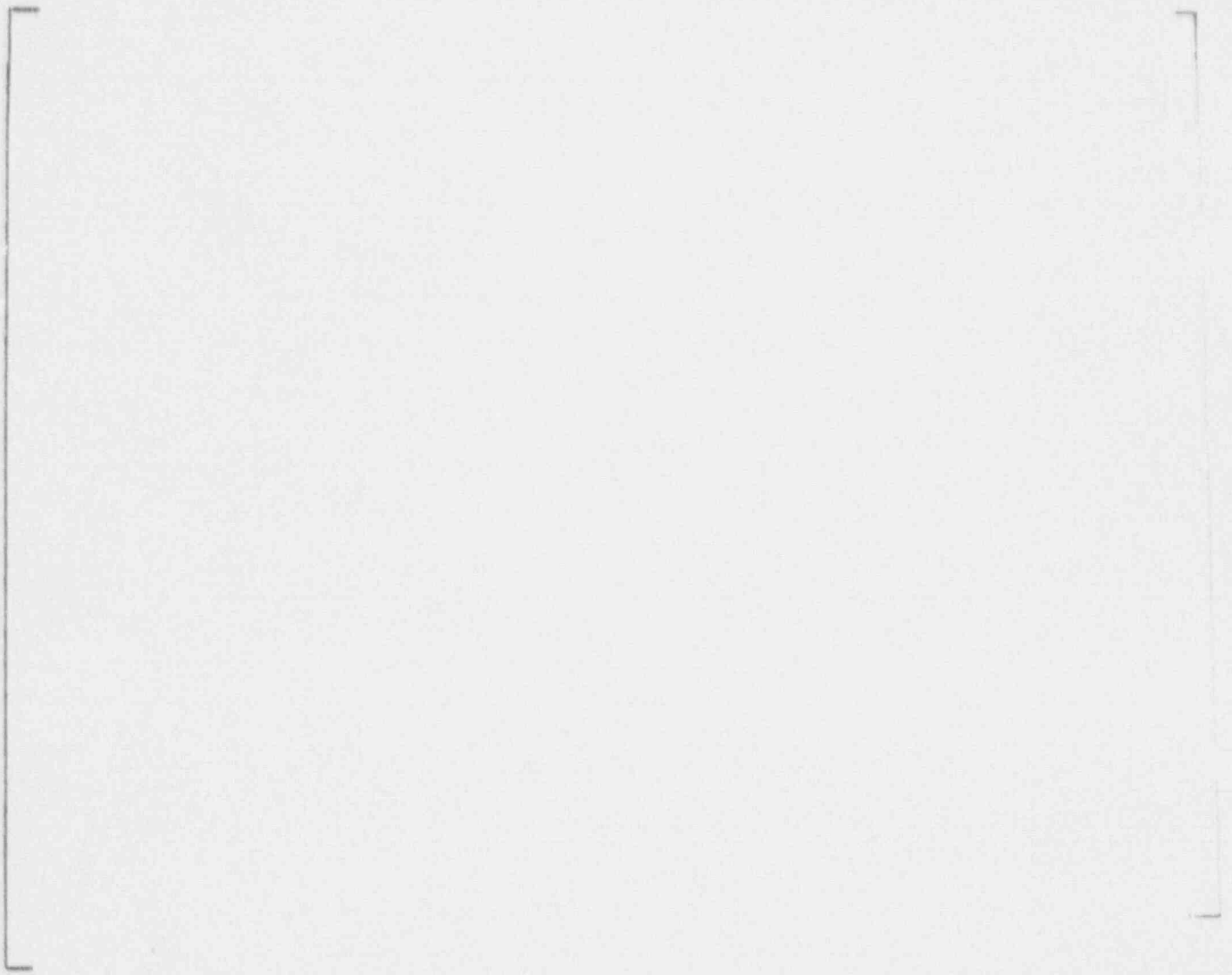

Figure 5-10. Critical Flaw Size Prediction for the Comanche Peak Nuclear Power Plant Node 2900 - SAW

SECTION 6.0
ASSESSMENT OF FATIGUE CRACK GROWTH

The purpose of the fatigue crack growth (FCG) analysis is to demonstrate that a postulated flaw will not grow through the wall under all operational loadings.

The fatigue crack growth in the Comanche Peak Unit 2 Nuclear Power Plant 10" accumulator lines was determined by comparison with a generic fatigue crack growth analysis of a similar piping system. The accumulator lines extending from the RCS cold leg injection points to the tank compare reasonably well with the generic analysis, having essentially the same geometry, materials, and fatigue crack growth rate. Based on comparing all parameters critical to the fatigue crack growth analysis, it was concluded that the generic analysis would envelop their fatigue crack growth. The details of the generic fatigue crack growth analysis are presented in appendix B. Fatigue crack growth results are summarized in table B-4 of appendix B.

Due to similarities in Westinghouse PWR designs it was possible to perform a generic fatigue crack growth calculation which would be applicable to many plants. A comparison was made of stresses, number of cycles, materials, and geometry.

The following summarizes the parameters which were compared:

Critical Location	Generic Cold Leg Nozzle To Pipe Weld	Comanche Peak Unit 2 Cold Leg Nozzle to Pipe Weld
Pipe Outer Diameter	10.75"	10.75"
Thickness	0.895"	.875"
Material	Austenitic Stainless Steel	Austenitic Stainless Steel
Normal Temperature	550°F	550°F
Normal Pressure	2235 psig	2235 psig
Normal Operating Stress (Press, DW, Thermal Exp.)	10.1 ksi	10.6 ksi
Thermal Transients	See Appendix B	*

* Thermal transient loadings are nearly identical for this comparison.

The maximum allowable preservice indication may have a depth of about 0.1 in. per IWB-3514.3, Allowable Indication Standard or Austenitic Piping, ASME Code, Section XI - Division 1, 1983 edition. Typical fatigue crack growth results for various initial flaw depths are given in Table B-4 in Appendix B. From the table an initial crack 0.10 inch deep is calculated to grow a depth of 0.132 in. at end of life. Similarly a crack having an initial depth of 0.15 in. grows to 0.186 in.

In conclusion, the fatigue crack growths calculated for the generic case, as summarized in section B.2.2, are applicable to the Comanche Peak Unit 2 Nuclear Power Plant accumulator lines. These results demonstrate that no significant fatigue crack growth will occur over the 40 year plant design life.

SECTION 7.0
ASSESSMENT OF MARGINS

In the preceding sections, the leak rate calculations, fracture mechanics analyses and fatigue crack growth assessment were performed. Margins at the critical locations are summarized in Table 7-1.

In summary, relative to

1. Flaw Size

   A margin of at least 2 exists between the critical flaws and the flaws yielding a leak rate of 10 gpm.

2. Leak Rate

   For the reference flaw sizes a margin of 10 exists between the calculated leak rate and the 1 gpm leak detection criteria of Regulatory Guide 1.45.

In the evaluation, the leak-before-break methodology is applied conservatively. The conservatisms used in the evaluation are summarized in Table 7-2.

TABLE 7-1

LEAKAGE FLAW SIZES, CRITICAL FLAW SIZES AND MARGINS

[ ] a,c,e

(a) For the cast injection nozzles, J_{app} was less than J_{max} and T_{app} was less than T_{mat} for a flaw having a length of [ ]^{a,c,e}.

TABLE 7-2

LBB CONSERVATISMS

- Factor of 10 on Leak Rate
- Factor of 2 on Leakage Flaw for all cases
- Algebraic Sum of Loads for Leakage
- Absolute Sum of Loads for Stability
- Average Material Strengths for Leakage
- Minimum Material Strengths for Stability

SECTION 8.0
CONCLUSIONS

This report justifies the elimination of 10" accumulator lines pipe breaks from the structural design basis for the Comanche Peak Unit 2 Nuclear Power Plant as follows:

a. Stress corrosion cracking is precluded by use of fracture resistant materials in the pipe system and controls on reactor coolant chemistry, temperature, pressure, and flow during normal operation.

b. Water hammer should not occur in the RCS piping (primary loop and the attached auxiliary lines) because of system design, testing, and operational considerations.

c. The effects of low and high cycle fatigue on the integrity of the accumulator line piping are negligible.

d. Adequate margin exists between the leak rate of small stable flaws and the capability of the Comanche Peak Unit 2 plant's reactor coolant system pressure boundary leakage detection system.

e. Ample margin exists between the small stable flaw sizes of item d and the critical flaws.

The postulated reference flaws will be stable because of the ample margins in d and e and will leak at detectable rates which will assure a safe plant shutdown.

Based on the above, it is concluded that pipe breaks in the 10" accumulator lines need not be considered in the structural design basis of the Comanche Peak Unit 2 Nuclear Power Plant.

APPENDIX A

LIMIT MOMENT

The internal stress system at the crack plane has to be in equilibrium with the applied loading, i.e., the hydrostatic pressure P, axial force F, and the bending moment M_b. The angle ß which identifies the point of stress inversion follows from the equilibrium of horizontal forces (see Figure A-1). That is:

a,c,e

Figure A-1. Pipe with a Through-Wall Crack in Bending

APPENDIX B

FATIGUE CRACK GROWTH CONSIDERATIONS

B.1 Thermal Transient Stress Analysis

The thermal transient stress analysis was performed for a typical PWR plant to obtain the through wall stress profiles for use in the fatigue crack growth analysis of Section B.2. The through wall stress distribution for each transient was calculated for i) the time corresponding to the maximum inside surface stress and, ii) the time corresponding to the minimum inside surface stress. These two stress profiles are called the maximum and minimum through wall stress distribution, respectively for convenience. The constant stresses due to pressure, deadweight and thermal expansion (at normal operating temperature, 550°F) loadings were superimposed on the through wall cyclical stresses to obtain the total maximum and minimum stress profile for each transient. Linear through wall stress distributions were calculated by conservative simplified methods for all minor transients. More accurate nonlinear through wall stress distributions were developed for severe transients by [ ]^{a,c,e}

B.1.1 Critical Location for Fatigue Crack Growth Analysis

The accumulator line design thermal transients (Section B.1.2), 1-D analysis data on accumulator line thermal transient stresses (based on ASME Section III NB3600 rules) and the geometry were reviewed to select the worst location for the fatigue crack growth analysis. [

]^{a,c,e} This location is selected as the worst location based on the following considerations:

i) the fatigue usage factor is highest.
ii) the stress due to thermal expansion is high.
iii) the effect of discontinuity due to the undercut at the weld will tend to increase the cyclical thermal transient loads.

iv) the review of data shows that the 1-D thermal transient stresses in the accumulator line pipi~~n~~ section are generally higher near the [RCL cold leg nozzle compared to rest of the accumulator line.]^{a,c,e}

B.1.2 Design Transients

The transient conditions selected for this evaluation are based on conservative estimates of the magnitude and the frequency of the temperature fluctuations resulting from various operating conditions in the plant. These are representative of the conditions which are considered to occur during plant operation. The fatigue evaluation based on these transients provides confidence that the component is appropriate for its application over the design life of the plant. All the normal operating and upset thermal transients, in accordance with design specification and the applicable system design criteria document (B-1), were considered for this evaluation. Out of these, only [

]^{a,c,e} These transients were selected on the basis of the following criteria:

[(B.1)

(B.2)

]^{a,c,e}

B.1.3 Simplified Stress Analysis

The simplified analysis method was used to develop conservative maximum and minimum linear through wall stress distributions due to thermal transients. [

.]^{a,c,e} The inside surface stress was calculated by the following equation which is similar to the transient portion of ASME Section III NB3600, Eq. 11:

$$S_i = [\qquad]^{a,c,e} \tag{B.3}$$

where,

[ ]^{a,c,e}

[

]^{a,c,e} The maximum and minimum inside surface stresses were searched from the S_i values calculated for each time step of the transient solution.

The outside surface stresses corresponding to maximum and minimum inside stresses were calculated by the following equations:

$$S_{01} = [\qquad]^{a,c,e} \tag{B.7}$$

$$S_{02} = [\qquad]^{a,c,e} \tag{B.8}$$

where,

[ ]a,c,e

The material properties for the accumulator pipe [(SA376/P316)] and the RCL [

]a,c,e The values of E and a, at the normal operating temperature, provide a conservative estimation of the through wall thermal transient stresses as compared to room temperature properties. The following values were conservatively used, which represent the highest of the [ ]a,c,e materials:

[ ]a,c,e

The maximum and minimum linear through wall stress distribution for each thermal transient was obtained by [

]a,c,e The simplified analysis discussed in this section was performed for all minor thermal transients of [ ]a,c,e Nonlinear through wall stress profiles were developed for the remaining severe transients as explained in Section B.1.4. The inside and outside surface stresses calculated by simplified methods for the minor transients are shown in Table B-2. [

]a,c,e This figure shows that the simplified method provides more conservative crack growth.

B.1.4 Nonlinear Stress Distribution for Severe Transients

[

]^{a,c,e} As mentioned earlier, the accumulator line section near the [ ]^{a,c,e} is the worst location for fatigue crack growth analysis. A schematic of the accumulator line geometry at this location, is shown in Figure B-2. [

]^{a,c,e}

B.1.5 Total Stress for Fatigue Crack Growth

The total through wall stress at a section was obtained by superimposing the pressure load stresses and the stresses due to deadweight and thermal expansion (normal operating case) on the thermal transient stresses (of Table B-2 or the nonlinear stress distributions discussed in Section B.1.4). Thus, the total stress for fatigue crack growth at any point is given by the following equation:

Total Stress for Fatigue Crack Growth	=	Thermal Transient Stress	+	Stress Due to DW + Thermal Expansion	+	Stress Due to Internal Pressure	(B.9)

The envelope thermal expansion, deadweight and pressure loads for calculating the total stresses of Equation B.9 are summarized in Table B-3.

B.2 Fatigue Crack Growth Analysis

The fatigue crack growth analysis was performed to determine the effect of the design thermal transients given in Table B-1. The analysis was performed for the critical cross section of the model which is identified in Figure B-2. A range of crack depths was postulated, and each was subjected to the transients in Table B-1.

B.2.1 Analysis Procedure

The fatigue crack growth analyses presented herein were conducted in the same manner as suggested by Section XI, Appendix A of the ASME Boiler and Pressure Vessel Code. The analysis procedure involves assuming an initial flaw exists at some point and predicting the growth of that flaw due to an imposed series of stress transients. The growth of a crack per loading cycle is dependent on the range of applied stress intensity factor ΔK_I, by the following relation:

$$\frac{da}{dN} = C_o \Delta K_I^n \qquad \text{(B-10)}$$

where "Co" and the exponent "n" are material properties, and ΔK_I is defined later, in equation (B-10). For inert environments these material properties are constants, but for some water environments they are dependent on the level of mean stress present during the cycle. This can be accounted for by adjusting the value of "Co" and "n" by a function of the ratio of minimum to maximum stress for any given transient, as will be discussed later. Fatigue crack growth properties of stainless steel in a pressurized water environment have been used in the analysis.

The input required for a fatigue crack growth analysis is basically the information necessary to calculate the parameter ΔK_I, which depends on crack and structure geometry and the range of applied stresses in the area where the crack exists. Once ΔK_I is calculated, the growth due to that particular cycle can be calculated by Equation (B.10). This increment of growth is then added to the original crack size, the ΔK_I adjusted, and the analysis proceeds to the next transient. The procedure is continued in this manner until all the transients have been analyzed.

The crack tip stress intensity factors (K_I) to be used in the crack growth analysis were calculated using an expression which applies for a semi-elliptic surface flaw in a cylindrical geometry (B-4).

The stress intensity factor expression was taken from reference B-4 and was calculated using the actual stress profiles at the critical section. The maximum and minimum stress profiles corresponding to each transient were input, and each profile was fit by a third order polynomial:

$$\sigma(x) = A_0 + A_1 \frac{x}{t} + A_2 \left(\frac{x}{t}\right)^2 + A_3 \left(\frac{x}{t}\right)^3 \qquad \text{(B-11)}$$

The stress intensity factor $K_I(d)$ was calculated at the deepest point of the crack using the following expression:

[ ]^{a,c,e} (B-12)

[ ]a,c,e

Calculation of the fatigue crack growth for each cycle was then carried out using the reference fatigue crack growth rate law determined from consideration of the available data for stainless steel in a pressurized water environment. This law allows for the effect of mean stress or R ratio (K_{Imin}/K_{Imax}) on the growth rates.

The reference crack growth law for stainless steel in a pressurized water environment was taken from a collection of data (B-5) since no code curve is available, and it is defined by the following equation:

$$\frac{da}{dN} = [\quad]^{a,c,e} \qquad \text{(B-13)}$$

where $K_{eff} = (K_{Imax})\ (1-R)^{1/2}$

$$R = \frac{K_{Imin}}{K_{Imax}}$$

$\frac{da}{dN}$ = crack growth rate in micro-inches/cycle

B.2.2 Results

Fatigue crack growth analyses were carried out for the critical cross section. Analysis was completed for a range of postulated flaw sizes oriented circumferentially, and the results are presented in Table B-4. The postulated flaws are assumed to be six times as long as they are deep. Even for the largest postulated flaw of [ ]^{a,c,e} the result shows that the flaw growth through the wall will not occur during the 40 year design life of the plant. For smaller flaws, the flaw growth is significantly lower. For example, a postulated [ ]^{a,c,e} inch deep flaw will grow to [ ]^{a,c,e} which is less than [ ]^{a,c,e} the wall thickness. These results also confirm operating plant experience. There have been no leaks observed in Westinghouse PWR accumulator lines.

B.3 REFERENCES

B-1 [Westinghouse System Standard Design Criteria 1.3, "Nuclear Steam Supply System Design Transients," Revision 2, April 15, 1974.]^{a,c,e}

B-2 ASME Section III, Division 1-Appendices, 1983 Edition, July 1, 1983.

B-3 WECAN -- Westinghouse Electric Computer Analysis, User's Marual -- Volumes 1, II, III and IV, Westinghouse Center, Pittsburgh, PA, Third Edition, 1982.

B-4 McGowan, J. J. and Raymund, M., "Stress Intensity Factor Solutions for Internal Longitudinal Semi-Elliptical Surface Flaws in a Cylinder Under Arbitrary Loadings", Fracture Mechanics ASTM STP 677, 1979, pp. 365-380.

B-5 Bamford, W. H., "Fatigue Crack Growth of Stainless Steel Reactor Coolant Piping in a Pressurized Water Reactor Environment", ASME Trans. Journal of Pressure Vessel Technology, February 1979.

TABLE B-1

THERMAL TRANSIENTS CONSIDERED FOR FATIGUE CRACK GROWTH EVALUATION

a,c,e

TABLE 3-2

STRESSES FOR THE MINOR TRANSIENTS (PSI)

TRANSIENT NO.	NO. OF CYCLES	MAXIMUM INSIDE STRESS	CORRESPONDING OUTSIDE STRESS	MINIMUM INSIDE STRESS	CORRESPONDING OUTSIDE STRESS
[					] a,c,e

TABLE B-3

ENVELOPE NORMAL LOADS

[a,c,e]

TABLE B-4

ACCUMULATOR LINE FATIGUE CRACK GROWTH RESULTS

Wall Thickness = [0.895 in.] a,c,e

[

]

[ ] a,c,e

Figure B-1 Comparison of Typical Maximum and Minimum Stress Profiles Computed by Simplified [ ]a,c,e

1. [ ]a,c,e
2. [ ]

[ ]a,c,e

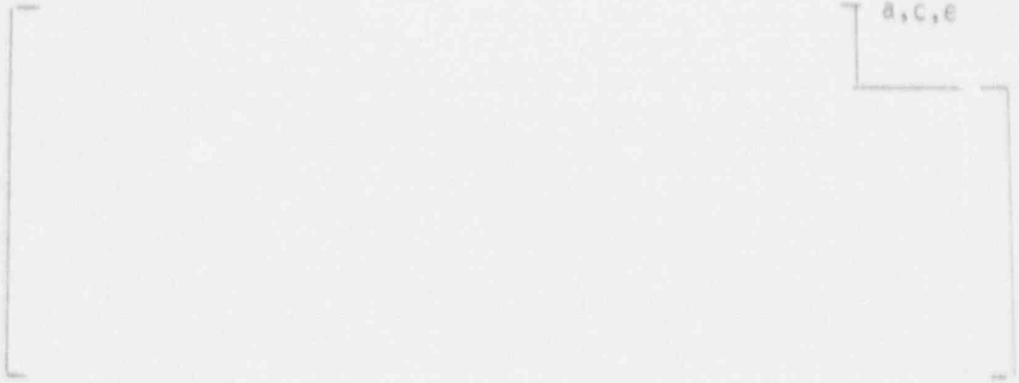

Figure B-2 Typical Schematic of Accumulator Line At [ ]a,c,e

Note: The minimum stress is zero through the thickness.

Figure B-3 [ ]^{a,c,e} Maximum and Minimum Stress Profiles for Transient #10

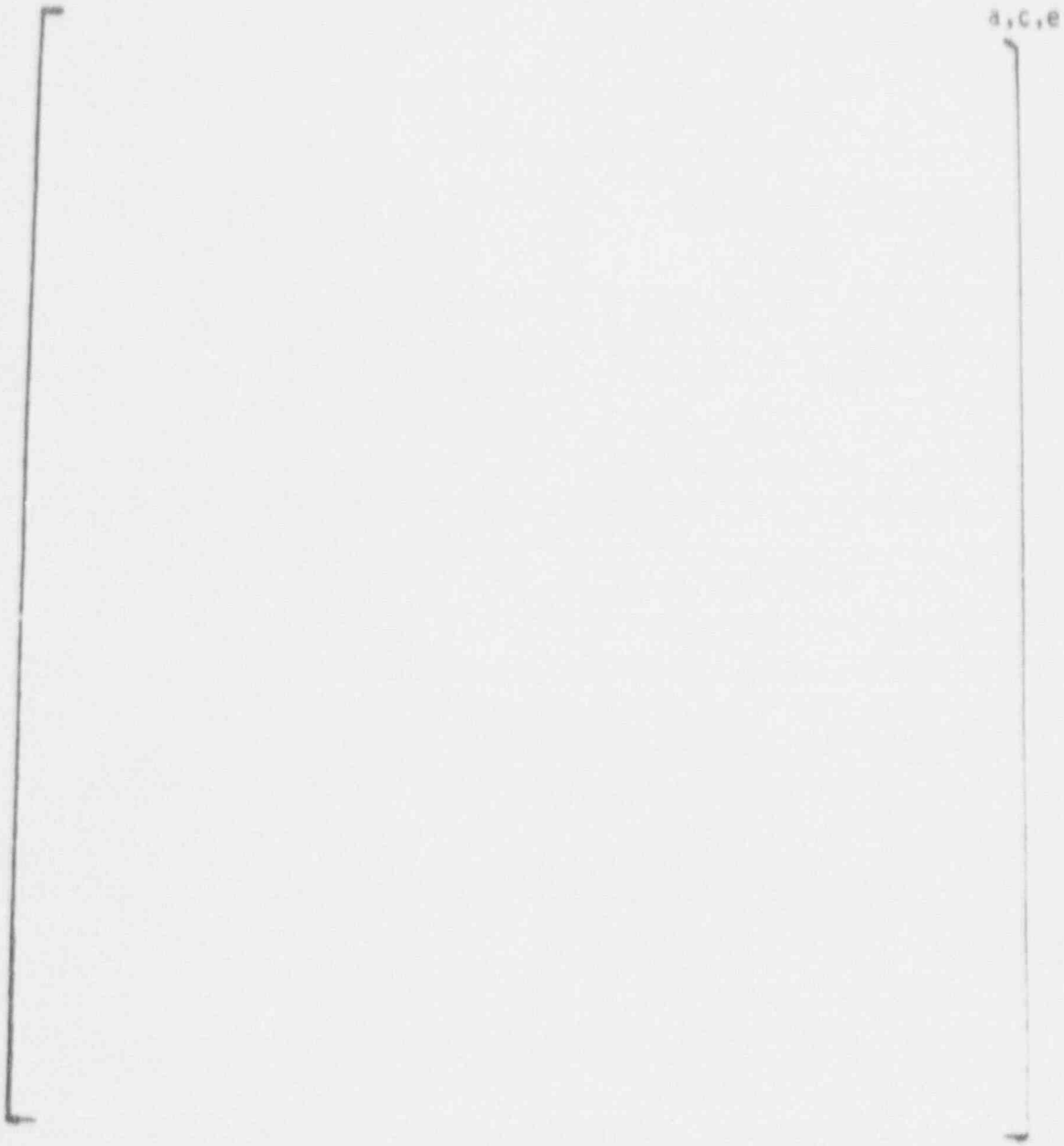

Figure B-4 [ ]^{a,c,e} Maximum and Minimum Stress Profiles for Transient #11

[ ]a,c,e

Figure B-5 [ ]a,c,e Maximum and Minimum Stress Profiles for Transient #12

Figure B-6 [ ]^{a,c,e} Maximum and Minimum Stress Profiles for Transient #14